

JONES-WENZL IDEMPOTENTS FOR RANK 2 SIMPLE LIE ALGEBRAS

DONGSEOK KIM

ABSTRACT. Temperley-Lieb algebras have been generalized to web spaces for rank 2 simple Lie algebras. Using these webs, we find a complete description of the Jones-Wenzl idempotents for the quantum $\mathfrak{sl}(3)$ and $\mathfrak{sp}(4)$ by single clasp expansions. We discuss applications of these expansions.

1. INTRODUCTION

After the discovery of the Jones polynomial [8, 9], its generalizations have been studied in many different ways. Using the quantum $\mathfrak{sl}(2)$ representation theory, the Jones polynomial can be seen as a polynomial invariant of a colored link whose components are colored by the two dimensional vector representation of the quantum $\mathfrak{sl}(2)$. By using all irreducible representations of the quantum $\mathfrak{sl}(2)$, one can find the colored Jones polynomial and it has been extensively studied [5, 11, 20, 25, 35, 38].

The other direction is to use the representation theory of other complex simple Lie algebras from the original work of Reshetikhin and Turaev [30, 31]. These quantized simple Lie algebras invariants can be found by using the Jones-Wenzl idempotents and fundamental representations. In this philosophy, Kuperberg introduced web spaces of simple Lie algebras of rank 2, $\mathfrak{sl}(3)$, $\mathfrak{sp}(4)$ and G_2 as generalizations of Temperley-Lieb algebras corresponding to $\mathfrak{sl}(2)$ [16]. Then he successively generalized the result for $\mathfrak{sl}(2)$ [32] that the dimension of the invariant subspace of the tensor of irreducible representations of the quantum $\mathfrak{sl}(3)$ and $\mathfrak{sp}(4)$ is equal to the dimension of web spaces of the given boundary with respect to the relations in Figure 5 and Figure 14 respectively [16]. But there was no immediate generalization to other Lie algebras until a new result for $\mathfrak{so}(7)$ [37] and $\mathfrak{sl}(4)$ [19]. The quantum $\mathfrak{sl}(3)$ invariants have many interesting results [1, 2, 12, 18, 28, 33] also have been generalized to the quantum $\mathfrak{sl}(n)$ [10, 21, 26, 34, 39]. An excellent review can be found in [6].

Ohtsuki and Yamada generalized Jones-Wenzl idempotents (these were called *magic weaving elements*) for the quantum $\mathfrak{sl}(3)$ web spaces by taking the expansions in Proposition 3.1 and 3.5 as a definition of clasps [28]. On the other hand, Kuperberg abstractly proved the existence of generalized Jones-Wenzl idempotents for other simple Lie algebras of rank 2, he called *clasps* [16]. In the recursive formula in Figure 1, the resulting webs have two (one with one clasp) clasps, thus it is called a *double clasps expansion* of the clasp of weight n . There is an expansion for which each resulting web has just one clasp as in Figure 3 [5]. We called it a *single clasp expansion* of the clasp of weight n . These expansions are very powerful tools for graphical calculus [5, 13, 35]. We provide single clasp expansions of all quantum $\mathfrak{sl}(3)$ clasps together with double, quadruple clasps expansions of all quantum $\mathfrak{sl}(3)$ clasps. We also find single and double clasp expansions of some quantum $\mathfrak{sp}(4)$ clasps.

2000 *Mathematics Subject Classification.* Primary 57M27; Secondary 57M25, 57R56.

The author was supported in part by KRF Grant M02-2004-000-20044-0.

Using expansions of clasps, Lickorish first found a quantum $\mathfrak{sl}(2)$ invariants of 3-manifolds [23, 24]. Ohtsuki and Yamada did for the quantum $\mathfrak{sl}(3)$ [28] and Yokota found for the quantum $\mathfrak{sl}(n)$ [39]. For applications of single clasp expansions, first we provide a criterion which determine the periodicity of a link using colored quantum $\mathfrak{sl}(3)$ and $\mathfrak{sp}(4)$ link invariants. We discuss a generalization of $3j, 6j$ symbols for the quantum $\mathfrak{sl}(3)$ representation theory. At last, we review how $\mathfrak{sl}(3)$ invariants extend for a special class of graphs.

The outline of this paper is as follows. In section 2, we review the original Jones-Wenzl idempotents and provide some algebraic background of the representation theory of $\mathfrak{sl}(3)$ and $\mathfrak{sp}(4)$. We provide single clasp expansions of all clasps for the quantum $\mathfrak{sl}(3)$ in section 3. In section 4 we study single clasp expansions of some clasps for the quantum $\mathfrak{sp}(4)$. In section 5, we will discuss some applications of the quantum $\mathfrak{sl}(3)$ clasps and their single clasp expansions. In section 6, we prove two key lemmas.

A part of the article is from the author's Ph. D. thesis. Precisely, section 3 and 6 are from [13, section 2.3] and section 4 is from [13, section 2.4].

Acknowledgements The author would like to thank Greg Kuperberg for introducing the subject and advising the thesis, Mikhail Khovanov, Jaeun Lee and Myungsoo Seo for their attention to this work. Also, the referee has been very helpful and critical during refereing and revising. The \TeX macro package PSTricks [29] was essential for typesetting the equations and figures.

2. JONES-WENZL IDEMPOTENTS AND ALGEBRAIC BACK GROUND

For standard terms and notations for representation theory, we refer to [4].

2.1. Jones-Wenzl idempotents. An explicit algebraic definition of Jones-Wenzl idempotents can be found in [5]. We will recall a definition of Jones-Wenzl idempotents which can be generalized for other simple Lie algebras. Let T_n be the n -th Temperley-Lieb algebra with generators, $1, e_1, e_2, \dots, e_{n-1}$, and relations,

$$\begin{aligned} e_i^2 &= -(q^{\frac{1}{2}} + q^{-\frac{1}{2}})e_i, \\ e_i e_j &= e_j e_i \quad \text{if } |i - j| \geq 2, \\ e_i &= e_i e_{i\pm 1} e_i. \end{aligned}$$

For each n , the algebra T_n has an idempotent f_n such that $f_n x = x f_n = \epsilon(x) f_n$ for all $x \in T_n$, where ϵ is an augmentation. These idempotents were first discovered by Jones [8] and Wenzl [36]. They found a recursive formula:

$$f_n = f_{n-1} + \frac{[n-1]}{[n]} f_{n-1} e_{n-1} f_{n-1},$$

as in Figure 1 where we use a rectangular box to represent f_n and the quantum integers are defined as

$$[n] = \frac{q^{\frac{n}{2}} - q^{-\frac{n}{2}}}{q^{\frac{1}{2}} - q^{-\frac{1}{2}}}.$$

Thus, they are named *Jones-Wenzl idempotents (projectors)*. It has the following properties 1) it is an idempotent 2) $f_n e_i = 0 = e_i f_n$ where e_i is a U-turn from the i -th to the $i + 1$ -th

$$\begin{array}{c} n \\ \hline n \end{array} = \begin{array}{c} n-1 \\ \hline n-1 \end{array} + \frac{[n-1]}{[n]} \begin{array}{c} n-1 \\ \hline n-2 \\ \hline n-1 \end{array}$$

FIGURE 1. A double clasps expansion of the clasp of weight n .

$$n - \text{[vertical bar]}^n - \text{[vertical bar]} - n = n - \text{[vertical bar]} - n \quad , \quad n - \text{[vertical bar]}^k - \text{[vertical bar]}^{n-k-2} = 0$$

FIGURE 2. Properties of the Jones-Wenzl idempotents.

$$\begin{array}{c} n \\ | \\ \text{---} \\ | \\ n \end{array} = \begin{array}{c} n-1 \\ | \\ \text{---} \\ | \\ n-1 \end{array} + \sum_{i=2}^n \frac{[n+1-i]}{[n]} \begin{array}{c} i & 1 \\ | & | \\ | & | \\ | & | \\ | & | \\ \text{---} & | \\ | & | \\ n-1 & \end{array}$$

FIGURE 3. A single clasp expansion of the clasp of weight n .

string as in Figure 2. The second property is called *the annihilation axiom*. We will discuss the importance of Jones-Wenzl idempotents in section 2.4.

2.2. The representation theory of $\mathfrak{sl}(3)$. The Lie algebra $\mathfrak{sl}(3)$ is the set of all 3×3 complex matrices with trace zero, which is an 8 dimensional vector space with the Lie bracket. Let λ_i be a fundamental dominant weight of $\mathfrak{sl}(3)$. All finite dimensional irreducible representation of $\mathfrak{sl}(3)$ are determined by its highest weight $\lambda = a\lambda_1 + b\lambda_2$, denoted by V_λ where a and b are all nonnegative integers. We will abbreviate $V_{a\lambda_1+b\lambda_2}$ by $V(a, b)$. The dimension and the quantum dimension of the fundamental representation $V_{\lambda_1} \cong (V_{\lambda_2})^*$ of $\mathfrak{sl}(3)$ are 3, [3]. The weight space of a fundamental representation $V(1, 0)$ is $[1, 0]$, $[-1, 1]$ and $[0, -1]$. The weight space of a fundamental representation $V(0, 1)$ is $[0, 1]$, $[1, -1]$ and $[-1, 0]$. Thus, one can easily find the following decomposition formula for a tensor product of a fundamental representation and an irreducible representation,

$$\begin{aligned} V_{\lambda_1} \otimes V_{a\lambda_1+b\lambda_2} &\cong V_{(a+1)\lambda_1+b\lambda_2} \oplus V_{(a-1)\lambda_1+(b+1)\lambda_2} \oplus V_{a\lambda_1+(b-1)\lambda_2}, \\ V_{\lambda_2} \otimes V_{a\lambda_1+b\lambda_2} &\cong V_{a\lambda_1+(b+1)\lambda_2} \oplus V_{(a+1)\lambda_1+(b-1)\lambda_2} \oplus V_{(a-1)\lambda_1+b\lambda_2}, \end{aligned}$$

with a standard reflection rule, a refined version of the Brauer's theorem [7, pp.142]. Using these tensor rules, one can find the following lemma.

Lemma 2.1. *For integers $a, b \geq 1$,*

$$\dim(\text{Inv}(V_{\lambda_1}^{\otimes a} \otimes V_{\lambda_2}^{\otimes b} \otimes V_{(b-1)\lambda_1+a\lambda_2})) = ab.$$

To compare the weight of cut paths and clasps, we recall the usual partial ordering of the weight lattice of $\mathfrak{sl}(3)$ as

$$\begin{aligned} a\lambda_1 + b\lambda_2 &\succ (a+1)\lambda_1 + (b-2)\lambda_2, \\ a\lambda_1 + b\lambda_2 &\succ (a-2)\lambda_1 + (b+1)\lambda_2. \end{aligned}$$

2.3. The representation theory of $\mathfrak{sp}(4)$. The Lie algebra $\mathfrak{sp}(4)$ is the set of all 4×4 complex matrices of the following form,

$$\begin{bmatrix} A & B \\ C & -{}^tA \end{bmatrix}, \text{ where } {}^tB = B, {}^tC = C$$

which is a 10 dimensional vector space with the Lie bracket, where A, B and C are 2×2 matrices. Let λ_i be a fundamental dominant weight of $\mathfrak{sp}(4)$. All finite dimensional irreducible representation of $\mathfrak{sp}(4)$ are determined by its highest weight $\lambda = a\lambda_1 + b\lambda_2$, denoted by V_λ where a and b are all nonnegative integers. We will abbreviate $V_{a\lambda_1+b\lambda_2}$ by $V(a, b)$. The dimension and the quantum dimension of the fundamental representation $V_{\lambda_1}(V_{\lambda_2})$ of $\mathfrak{sp}(4)$ are 4, $[4](5, [5]$, respectively). The weight space of a fundamental representation $V(1, 0)$ is $[1, 0]$, $[-1, 1]$, $[1, -1]$ and $[-1, 0]$. The weight space of a fundamental representation $V(0, 1)$ is $[0, 1]$, $[0, -1]$, $[2, -1]$, $[-2, 1]$ and $[0, 0]$. Thus, one can easily find the following decomposition formula for a tensor product of a fundamental representation and an irreducible representation,

$$V_{\lambda_1} \otimes V_{a\lambda_1+b\lambda_2} \cong V_{(a+1)\lambda_1+b\lambda_2} \oplus V_{(a-1)\lambda_1+(b+1)\lambda_2} \oplus V_{(a+1)\lambda_1+(b-1)\lambda_2} \oplus V_{(a-1)\lambda_1+b\lambda_2},$$

$$V_{\lambda_2} \otimes V_{a\lambda_1+b\lambda_2} \cong V_{a\lambda_1+(b+1)\lambda_2} \oplus V_{a\lambda_1+(b-1)\lambda_2} \oplus V_{(a-2)\lambda_1+(b+1)\lambda_2} \oplus V_{(a+2)\lambda_1+(b-1)\lambda_2} \oplus V_{a\lambda_1+b\lambda_2},$$

with a similar reflection rule. Using these tensor rules, one can find the following two lemmas.

Lemma 2.2. *For positive integer n ,*

$$\dim(\text{Inv}(V_{\lambda_1}^{\otimes n+1} \otimes V_{(n-1)\lambda_1})) = \frac{n(n+1)}{2}.$$

Lemma 2.3. *For positive integer n ,*

$$\dim(\text{Inv}(V_{\lambda_2}^{\otimes n+1} \otimes V_{(n-1)\lambda_2})) = \frac{n(n+1)}{2}.$$

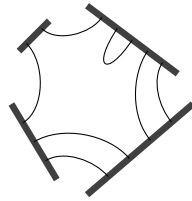
There is a natural partial ordering of the $\mathfrak{sp}(4)$ weight lattice given by

$$\begin{aligned} a\lambda_1 + b\lambda_2 &\succ (a-2)\lambda_1 + (b+1)\lambda_2, \\ a\lambda_1 + b\lambda_2 &\succ (a+2)\lambda_1 + (b-2)\lambda_2. \end{aligned}$$

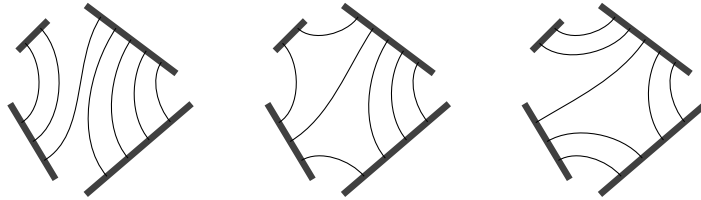
2.4. Invariant vector spaces and Web spaces. In this subsection, we briefly review the web spaces, full details can be found in [16]. Let V_i be an irreducible representation of complex simple Lie algebras \mathfrak{g} . One of classical invariant problems is to characterize the vector space of invariant tensors

$$\text{Inv}(V_1 \otimes V_2 \otimes \dots \otimes V_n),$$

together with algebraic structures such as tensor products, cyclic permutations and contractions. The dimension of such a vector space is given by Cartan-Weyl character theory; $\dim(\text{Inv}(V_1 \otimes V_2 \otimes \dots \otimes V_n))$ is the number of copies of the trivial representation in the decomposition of $V_1 \otimes V_2 \otimes \dots \otimes V_n$ into irreducible representations. For this algebraic space, we look for a geometric counterpart which can preserve the algebraic structure of the invariant spaces. The discovery of quantum groups opens the door for the link between invariant spaces and topological invariants of links and manifolds. For quantum $\mathfrak{sl}(2, \mathbb{C})$, the dimension of the invariant spaces of $V_1^{\otimes 2n}$ is the dimension of the n -th Temperley-Lieb algebra as a vector space which is generated by chord diagrams with $2n$ marked points on the boundary of the disk where V_1 is the vector representation of $\mathfrak{sl}(2, \mathbb{C})$. In particular, this space is free, *i.e.*, there is no relation between chord diagrams. To represent any irreducible representations other than the vector representation, we use Jones-Wenzl idempotents as we described in section 2.1. Then all webs in the web space of a tensor of irreducible representations $V_{i_1} \otimes V_{i_2} \otimes \dots \otimes V_{i_n}$ can be obtained from webs in the web space of $V_1^{\otimes \sum_k i_k}$ and by attaching Jones-Wenzl idempotents of weight i_k along the boundary (some webs become zero by the annihilation axiom, no longer a basis for web space and the other nonzero webs are called *basis webs*), where V_i is the irreducible representation of the quantum $\mathfrak{sl}(2, \mathbb{C})$ of highest weight i and $k = 1, 2, \dots, n$. For example [16], the web



is not a basis web of $V_2 \otimes V_3 \otimes V_4 \otimes V_5$, which instead has basis



where the Jones-Wenzl idempotents were presented by the thick gray lines instead of boxes.

A first generalization of Temperley-Lieb algebras was made for simple Lie algebras of rank 2, $\mathfrak{sl}(3, \mathbb{C})$, $\mathfrak{sp}(4, \mathbb{C})$ and G_2 [16]. Each diagrams appears in a geometric counterpart of the invariant vectors is called a web, precisely a directed and weighted cubic planar graph. Unfortunately, some of webs are no longer linearly independent for simple Lie algebra other than $\mathfrak{sl}(2, \mathbb{C})$. For example, we look at the web space of $\mathfrak{sl}(3, \mathbb{C})$ representations. Let V_{λ_1} be the vector representation of the quantum $\mathfrak{sl}(3, \mathbb{C})$ and V_{λ_2} be the dual representation of V_{λ_1} . The web space of a fixed boundary (a sequence of V_{λ_1} and V_{λ_2}) is a vector space spanned by the all webs of the given boundary which is generated by the webs in Figure 4 (as inward and outward arrows) modulo by the subspace spanned by the equation of diagrams which are called a complete set of the relations, equations 1, 2 and 3 shown in Figure 5. We have drawn a web in Figure 6. We might use the notation $+$, $-$ for V_{λ_1} , V_{λ_2} but it should be clear. For several reasons, such as the positivity and the integrality [22], we use $-[2]$ in relation 2 but one can use a quantum integer $[2]$ and get an independent result. If one uses $[2]$, one can rewrite all results in here by multiplying each trivalent vertex by the complex number i .

FIGURE 4. Generators of the quantum $\mathfrak{sl}(3)$ web space.

$$\begin{aligned}
 (1) \quad & \text{A circle with a clockwise arrow} = [3] \\
 (2) \quad & \text{A line with a loop (two arrows forming a circle) in the middle} = -[2] \text{ followed by a line with an arrow pointing left} \\
 (3) \quad & \text{A square with arrows on all four sides (top and bottom pointing right, left and right pointing left)} = \text{Two arcs (top and bottom) pointing left} + \text{Two arcs (left and right) pointing down}
 \end{aligned}$$

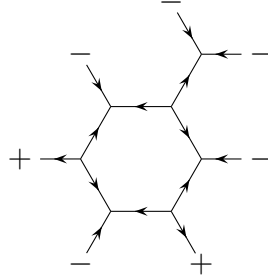
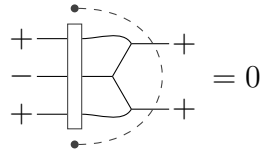
FIGURE 5. Complete relations of the quantum $\mathfrak{sl}(3)$ web space.FIGURE 6. An example of the webs with a boundary $(+ - + - - -)$.

FIGURE 7. An example of the annihilation axiom with a cut path.

To define the generalization of Jones-Wenzl idempotents, *clasps*, we first generalize the annihilation axiom for other web spaces. We need to introduce new concepts: a *cut path* is a path which is transverse to strings of a web, and the *weight* of a cut path is the sum of weights of all decorated strings which intersect with the cut path. For example, the weight of the clasp in Figure 7 is $2V_{\lambda_1}$ abbreviated by $(2, 0)$. Then we can generalize the annihilation

axiom as follows: if we attach the clasp to a web which has a cut path of a weight less than that of the clasp, then it is zero. Since the weight of the clasp in Figure 7 is $(2, 1)$ and there is a cut path of weight $(2, 0)$, the web in Figure 7 is zero by the annihilation axiom. For $\mathfrak{sl}(3, \mathbb{C})$, the clasp of weight (a, b) is the web in the web space of $V_{\lambda_1}^{\otimes a} \otimes V_{\lambda_2}^{\otimes b} \otimes (V_{\lambda_1}^*)^{\otimes a} \otimes (V_{\lambda_2}^*)^{\otimes b}$ which satisfies the annihilation axiom and the idempotent axiom. An algebraic proof of the existence of clasps for $\mathfrak{sl}(3)$ and $\mathfrak{sp}(4)$ is given [16]. On the other hand, the double clasps expansion and the quadruple clasps expansion formulae [28] do concretely show the existence of the $\mathfrak{sl}(3)$ clasp. Using these expansions one can find Example 2.4.

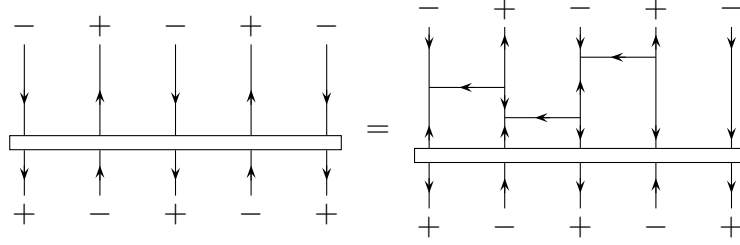
Example 2.4. *The complete expansions of the clasps of weight $(2, 0)$ and $(3, 0)$ are*

$$\begin{aligned} \text{Clasp}(2, 0) &= \text{web} + \frac{1}{[2]} \text{web} \\ \text{Clasp}(3, 0) &= \text{web} + \frac{[2]}{[3]} \left(\text{web} + \text{web} \right) + \frac{[1]}{[3]} \left(\text{web} + \text{web} \right) + \frac{1}{[2][3]} \text{web} \end{aligned}$$

3. SINGLE CLASP EXPANSIONS FOR THE QUANTUM $\mathfrak{sl}(3)$ CLASPS

First we look at a single clasp expansion of the clasp of weight $(n, 0)$ where the weight (a, b) stands for $a\lambda_1 + b\lambda_2$ in section 3.1. We can easily find a single clasp expansion of the clasp of weight $(0, n)$ by reversing arrows in the equation presented in Figure 4. In section 3.2, we find a single clasp expansion of the clasp of weight (a, b) and double clasps expansions.

3.1. Single clasp expansions of a clasp of weight $(n, 0)$. In Figure 4, one can easily see that there is no elliptic face (face of sizes less than six) for each web in the right hand side of the equation, thus they are linearly independent because there is no relation to be applied. If we set $a = (n + 1), b = 1$, we find the dimension of the web space of $V_{\lambda_1}^{\otimes n+1} \otimes V_{\lambda_2} \otimes V_{(n-1)\lambda_2}$ is n by Lemma 2.1. Therefore, a basis for the single clasp expansion can be given as in Figure 4. It is worth to mention that *i)* this expansion can be obtained from a complete expansion (linear expansions of webs without any clasps) which can be found by using a double clasps expansion iteratively [28] and then attaching a clasp of weight $(n - 1, 0)$ to each web in the expansion; *ii)* the single clasp expansion in Proposition 3.1 holds for any $\mathfrak{sl}(n)$ where $n \geq 4$ because $\mathfrak{sl}(3)$ is naturally embedded in $\mathfrak{sl}(n)$. By symmetries, there are four different single clasp expansions depending on where the clasp of weight $(n - 1, 0)$ is located. For the equation shown in Figure 4, the clasp is located at the southwest corner, which will be considered the standard expansion, otherwise, we will state the location of the clasp. For $n = 2$, the Proposition 3.1 is identical to Example 2.4 and for $n = 3$, we can easily verify the Proposition 3.1 from Example 2.4 by attaching the clasp of weight $(2, 0)$ to the southeast corner of each web in the complete expansion.

FIGURE 8. A non-segregated clasp of weight $(2, 3)$.

Proposition 3.1. *For positive integer n ,*

$$(4) \quad \begin{array}{c} n \\ \text{Diagram of } n \text{ vertical lines} \\ n \end{array} = \begin{array}{c} n-1 \\ \text{Diagram of } n-1 \text{ vertical lines} \\ n-1 \end{array} + \sum_{i=2}^n \frac{[n+1-i]}{[n]} \begin{array}{c} i \quad 1 \\ \text{Diagram of } n-1 \text{ vertical lines with a clasp} \\ n-1 \end{array}$$

Proof. If we attach a \wedge on the top of webs in the equation shown in Figure 4, the left side of the equation in Figure 4 becomes zero and all webs in the right side of the equation in Figure 4 become multiples of a web. Thus we get the following $n-1$ equations.

$$a_{n-1} - [2]a_n = 0.$$

For $i = 1, 2, \dots, n-2$,

$$a_i - [2]a_{i+1} + a_{i+2} = 0.$$

One can see that these equations are independent. By normalization, we get $a_1 = 1$. Then we check the answer in the proposition satisfies these equations. Since these webs in the equation depicted in Figure 4 form a basis, these coefficients are unique. \square

3.2. Single clasp expansions of a non-segregated clasp of weight (a, b) . The most interesting case is a single clasp expansion of the clasp of weight (a, b) where $a \neq 0 \neq b$. By Lemma 2.1, we know the number of webs in a single clasp expansion of the clasp of weight (a, b) is $(a+1)b$. We need a set of basis webs with a nice rectangular order, but we can not find one in the general case. Even if one finds such a basis, each web in the basis would have many hexagonal faces which make it very difficult to get numerical relations. So we start from an alternative, *non-segregated* clasp. A non-segregated clasp is obtained from the segregated clasp by attaching a sequence of H 's until we get the desired shape of edge orientations. Fortunately, there is a canonical way to find them by putting H 's from the leftmost string of weight λ_2 or $-$ until it reach to the desired position. The left side of the equation in Figure 8 is an example of a non-segregated clasp of weight $(2, 3)$. The right side of the equation in Figure 8 shows a sequence of H 's which illustrates how we obtain it from the segregated clasp of weight $(2, 3)$.

First of all, we can show that the non-segregated clasps are well-defined [13, Lemma 2.6]. One can prove that non-segregated clasps also satisfy two properties of segregated clasps: 1) two consecutive non-segregated clasps is equal to a non-segregated clasp, 2) if we attach a

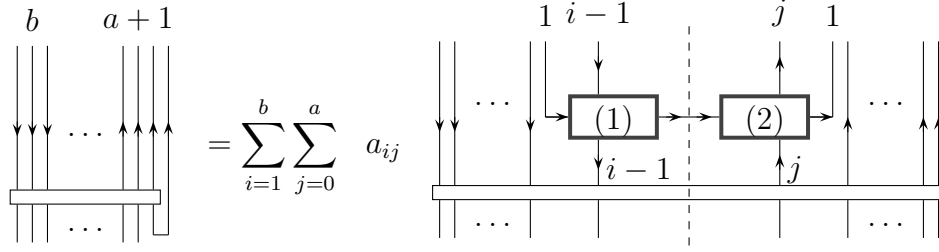
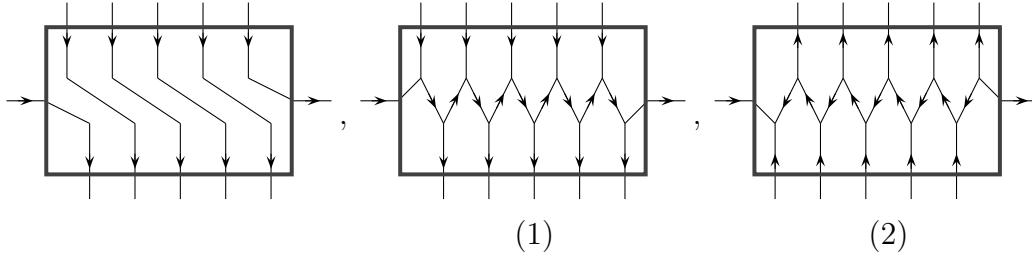
FIGURE 9. A single clasp expansion of a non-segregated clasp of weight (a, b) .

FIGURE 10. Fillings for the boxes in Figure 9.

web to a non-segregated clasp and if it has a cut path whose weight is less than the weight of the clasp, then it is zero [13, Lemma 2.7].

The equation shown in Figure 9 is a single clasp expansion of a non-segregated clasp of weight (a, b) , the webs in the right hand side of the equation form a basis because they are linearly independent (no elliptic faces) and their cardinality is the same as the dimension of the invariant space of $V_{a\lambda_1+(b-1)\lambda_2} \otimes V_{\lambda_1}^{\otimes a+1} \otimes V_{\lambda_2}^{\otimes b-1}$. Let us denote the web corresponding to the coefficient $a_{i,j}$ by $D_{i,j}$. Kuperberg showed that for a fixed boundary, the interior can be filled by a cut out from the hexagonal tiling of the plane with the given boundary [16]. For our cases, there are two possible fillings but we use the maximal cut out of the hexagonal tiling. We draw examples of the case $i = 6, j = 5$ and the first one in Figure 10 is not a maximal cut out and the second one is the maximal cut out which fits to the left rectangle and the last one is the maximal cut out which fits to the right rectangle as the number indicated in Figure 9. An example of a single clasp expansion of a segregated clasp of weight $(2, 2)$ can be found in [13, pp. 18]. We establish Lemma 3.2 first.

Lemma 3.2. *If we set $a_{1,0} = x$, then the coefficient $a_{i,j}$ in the equation presented in Figure 9 is*

$$\frac{[b-i+1][b+j+1]}{[b][b+1]}x.$$

Proof. First we attach a \wedge or a \cap to find one exceptional and three types of equations as follow.

$$[3]a_{1,0} - [2]a_{1,1} - [2]a_{2,0} + a_{2,1} = 0.$$

Type I : For $j = 0, 1, \dots, a$,

$$a_{b-1,j} - [2]a_{b,j} = 0.$$

Type II : For $i = 1, 2, \dots, b-2$ and $j = 0, 1, \dots, a$.

$$a_{i,j} - [2]a_{i+1,j} + a_{i+2,j} = 0.$$

Type III : For $i = 1, 2, \dots, b$ and $j = 0, 1, \dots, a-2$.

$$a_{i,j} - [2]a_{i,j+1} + a_{i,j+2} = 0.$$

First we can see that the right side of the equation shown in Figure 9 is a basis for a single clasp expansion because the number of webs in the expansion is equal to the dimension in Lemma 2.1 and none of these webs has any elliptic faces. Second we find that these equations has at least $(a+1)b$ independent equations. Then we plug in these coefficients to equations to check that they are the right coefficients. \square

Theorem 3.3. *The coefficient $a_{i,j}$ in the equation shown in Figure 9 is*

$$\frac{[b-i+1][b+j+1]}{[b][a+b+1]}.$$

Proof. Usually we normalize one basis web in the expansion to get a known value. But we can not normalize for this expansion yet because it is not a segregated clasp. Thus we use a complicate procedure in Lemma 6.2 to find that the coefficient of $a_{1,a}$ is 1. Then, we find that x in Lemma 3.2 is $\frac{[b+1]}{[a+b+1]}$ and it completes the proof of the theorem. \square

We find a double clasps expansion as shown in Theorem 3.4, the box between two clasps is filled by the unique maximal cut out from the hexagonal tiling with the given boundary as we have seen in Figure 10.

Theorem 3.4. *For $a, b \geq 1$,*

Proof. It follows from Lemma 6.1 and Lemma 6.2. \square

The expansion in equation depicted in Figure 11 was first used to define the segregated clasp of weight (a, b) [28]. The clasps can be constructed from web spaces [16] and these two are known to be equal. We will apply Theorem 3.3 to demonstrate the effectiveness of single clasp expansions by deriving the coefficients in the equation shown in Figure 11.

Proposition 3.5. [28] *The coefficient a_k in the equation portrayed in Figure 11 is*

$$(-1)^k \frac{[a]![b]![a+b-k+1]!}{[a-k]![b-k]![k]![a+b+1]}.$$

$$\begin{array}{c} a \\ \uparrow \\ \text{---} \\ \downarrow \\ b \end{array} = \sum_{k=0}^{\text{Min}(a,b)} a_k \begin{array}{c} a \quad b \\ \uparrow \quad \downarrow \\ \text{---} \quad \text{---} \\ \downarrow \quad \uparrow \\ a \quad b \end{array}$$

FIGURE 11. A quadruple clasps expansion of the segregated clasp of weight (a, b) .

$$\begin{array}{c} a \\ \uparrow \\ \text{---} \\ \downarrow \\ b \end{array} = \begin{array}{c} a \quad b \\ \uparrow \quad \downarrow \\ \text{---} \quad \text{---} \\ \downarrow \quad \uparrow \\ a \quad b \end{array} - \frac{[a]}{[a+b+1]} \begin{array}{c} a \quad b \\ \uparrow \quad \downarrow \\ \text{---} \quad \text{---} \\ \downarrow \quad \uparrow \\ a \quad b \end{array}$$

FIGURE 12. Induction step for the proof of Proposition 3.5.

Proof. Let us denote a basis web in the right side of equation 11 by $D(k)$ which is corresponding to the coefficient a_k . We induct on $a+b$. It is clear for $a=0$ or $b=0$. If $a \neq 0 \neq b$ then we use a segregated single clasp expansion of weight (a, b) in the middle for the first equality. Even if we do not use the entire single clasp expansion of a segregated clasp, once we attach clasps of weight $(a, 0), (0, b)$ on the top, there are only two nonzero webs which are webs with just one U -turn. One of resulting webs has some H 's as in Figure 12 but if we push them down to the clasp of weight $(a, b-1)$ in the middle, it becomes a non-segregated clasp. For the second equality we use a non-segregated single clasp expansion at the clasp of weight $(a, b-1)$ for which clasps of weight $(a-1, b-1)$ are located at northeast corner. By the induction hypothesis, we have

$$\begin{aligned}
&= \sum_{k=0}^{b-1} (-1)^k \frac{[a]![b-1]![a+b-k]!}{[a-k]![b-1-k]![k]![a+b]!} D(k) \\
&\quad - \frac{[a+1][a]}{[a+b+1][a+b]} \sum_{k=0}^{b-1} (-1)^k \frac{[a-1]![b-1]![a+b-1-k]!}{[a-1-k]![b-1-k]![k]![a+b-a]!} D(k+1) \\
&= 1 \cdot D(0) + \sum_{k=1}^{b-1} ((-1)^k \frac{[a]![b-1]![a+b-k]!}{[a-k]![b-1-k]![k]![a+b]!} \\
&\quad + (-1)^k \frac{[a+1]![b-1]![a+b-k]!}{[a-k]![b-1-k]![k-1]![a+b]!}) D(k) \\
&\quad - (-1)^{b-1} \frac{[a+1][a]}{[a+b+1][a+b]} \frac{[a-1]![b-1]![a]!}{[a-b]![0]![b-1]![a+b-1]!} D(b) \\
&= D(0) + \sum_{k=1}^{b-1} (-1)^k \frac{[a]![b]![a+b+1-k]!}{[a-k]![b-k]![k]![a+b+1]!} \left(\frac{[b-k][a+b+1] + [k][a+1]}{[b][a+b+1-k]} \right) D(k) \\
&\quad + (-1)^b \frac{[a]![b-1]![a+1]!}{[a-b]![0]![b-1]![a+b+1]!} D(b) \\
&= \sum_{k=0}^b (-1)^k \frac{[a]![b]![a+b+1-k]!}{[a-k]![b-k]![k]![a+b+1]!} D(k)
\end{aligned}$$

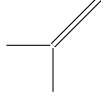
□

4. SINGLE CLASP EXPANSION FOR THE QUANTUM $\mathfrak{sp}(4)$

The quantum $\mathfrak{sp}(4)$ webs are generated by a single web in Figure 13 and a complete set of relations is given in Figure 14 [16]. Again, an algebraic proof of the existence of the clasp of the weight (a, b) using the annihilation axiom and the idempotent axiom is given in [16]. On the other hand, one can use the double clasps expansions in Corollary 4.2 and Corollary 4.4 to define the clasps of the weight $(n, 0)$ and $(0, n)$. Unfortunately, we do not have any expansion formula for the clasp of the weight (a, b) where $a \neq 0 \neq b$.

We can define tetravalent vertices to achieve the same end as in Figure 15. We will use these shapes to find a single clasp expansion otherwise there is an ambiguity of a preferred direction by the last relation presented in Figure 14. First we will find single clasp expansions of clasps of weight $(n, 0)$ and $(0, n)$ and then use them to find coefficients of double clasps expansions of clasps of weight $(n, 0)$ and $(0, n)$. But we are unable to find a single clasp expansion of the clasp of weight (a, b) where $a \neq 0 \neq b$. Remark that the cut weight is defined slightly different way. A cut path may cut diagonally through a tetravalent vertex, and its weight is defined as $n\lambda_1 + (k + k')\lambda_2$, where n is the number of type “1”, single strands, that it cuts, k is the number of type “2”, double strands, that it cuts, and k' is the number of tetravalent vertices that it bisects.

First we will look at a single clasp expansion of clasps of weight $(n, 0)$. By combining with the weight diagram of $V_{\lambda_1}^{\otimes n}$ and minimal cut paths, we can find a basis for single clasp expansion of a clasp of weight $(n, 0)$ as in Figure 16. Precisely, one can easily see that there is no elliptic face for each web in the right hand side of the equation in Figure 16, thus they

FIGURE 13. The generator of the quantum $\mathfrak{sp}(4)$ web space.

$$\begin{aligned}
 \bigcirc &= -\frac{[6][2]}{[3]}, & \bigcirc\bigcirc &= \frac{[6][5]}{[3][2]} \\
 \text{double line with a loop} &= 0, & \text{double line with a twist} &= -[2]^2 \text{double line} \\
 \text{triangle with double lines} &= 0, & \text{Y-junction} - \text{X-junction} &= \text{arc} - \text{arc}
 \end{aligned}$$

FIGURE 14. A complete set of relations of the quantum $\mathfrak{sp}(4)$ web space.

$$\begin{aligned}
 \text{X-junction} &= \text{Y-junction} - \text{arc}, & \text{double X-junction} &= \text{double Y-junction}
 \end{aligned}$$

FIGURE 15. Tetravalent vertices.

$$\begin{aligned}
 &\text{web with } n \text{ strands entering and } n \text{ exiting} \\
 &= \sum_{i=0}^{n-1} \sum_{j=i+1}^n a_{ij} \text{web with } n-1 \text{ strands and a clasp}
 \end{aligned}$$

FIGURE 16. A single clasp expansion of the clasp of weight $(n, 0)$.

are linearly independent. By Lemma 2.2, we know that the dimension of the web space of $V_{\lambda_1}^{\otimes n+1} \otimes V_{(n-1)\lambda_1}$ is $\frac{n(n+1)}{2}$. Thus, webs in right hand side of the equation form a basis. First, we will look at the case $n = 2$. First for $n = 2$, we set the following equation,

$$\text{web with a clasp} = a_{01} \text{two parallel strands} + a_{02} \text{X-junction} + a_{12} \text{two parallel strands with a loop}$$

If we attach a \cap on the top of webs, we have

$$0 = \text{web with a clasp and a cap} = a_{01} \text{two parallel strands with a cap} + a_{02} \text{X-junction with a cap} + a_{12} \text{two parallel strands with a cap and a loop} = (a_{01} + \frac{[6][2]}{[3]}a_{02} - \frac{[6][2]}{[3]}a_{12}) \text{two parallel strands with a cap}$$

We first find $a_{01} + \frac{[6][2]}{[3]}a_{02} - \frac{[6][2]}{[3]}a_{12} = 0$. Next we attach a \nearrow on the top of webs, we have

$$0 = \begin{array}{c} \nearrow \\ \text{web} \end{array} = a_{01} \begin{array}{c} \nearrow \\ | \end{array} + a_{02} \begin{array}{c} \nearrow \\ \diagdown \end{array} + a_{12} \begin{array}{c} \nearrow \\ \cup \end{array} = (a_{01} - [2]^2 a_{02}) \begin{array}{c} \nearrow \\ | \end{array}$$

By normalization, we get $a_{01} = 1$. Consequently, we find

$$a_{02} = \frac{1}{[2]^2}$$

$$a_{12} = \frac{[3]}{[6][2]}a_{01} + a_{02} = \frac{[3]}{[6][2]} + \frac{1}{[2]^2} = \frac{[4][3]}{[2]^2[6]}.$$

For $n = 3$, we set the following equation,

$$\begin{array}{c} \text{web} \end{array} = a_{01} \begin{array}{c} | \\ \text{web} \end{array} + a_{02} \begin{array}{c} \diagup \\ \text{web} \end{array} + a_{03} \begin{array}{c} \diagdown \\ \text{web} \end{array} + a_{12} \begin{array}{c} \cup \\ \text{web} \end{array} + a_{13} \begin{array}{c} \cap \\ \text{web} \end{array} + a_{23} \begin{array}{c} \text{web} \end{array}$$

If we attach a \nearrow on the leftmost top of webs, we have

$$0 = \begin{array}{c} \nearrow \\ \text{web} \end{array} = a_{01} \begin{array}{c} \nearrow \\ | \end{array} + a_{02} \begin{array}{c} \nearrow \\ \diagdown \end{array} + a_{03} \begin{array}{c} \nearrow \\ \diagup \end{array} + a_{12} \begin{array}{c} \nearrow \\ \cup \end{array} + a_{13} \begin{array}{c} \nearrow \\ \cap \end{array} + a_{23} \begin{array}{c} \nearrow \\ \text{web} \end{array}$$

We find

$$a_{12} + \frac{[6][2]}{[3]}a_{13} - \frac{[6][2]}{[3]}a_{23} = 0.$$

If we attach a \searrow on the rightmost top of webs, we have

$$0 = \begin{array}{c} \searrow \\ \text{web} \end{array} = a_{01} \begin{array}{c} \searrow \\ | \end{array} + a_{02} \begin{array}{c} \searrow \\ \diagup \end{array} + a_{03} \begin{array}{c} \searrow \\ \diagdown \end{array} + a_{12} \begin{array}{c} \searrow \\ \cup \end{array} + a_{13} \begin{array}{c} \searrow \\ \cap \end{array} + a_{23} \begin{array}{c} \searrow \\ \text{web} \end{array}$$

We obtain the second equation,

$$a_{01} + \frac{[6][2]}{[3]}a_{02} - [2][4]a_{03} - \frac{[6][2]}{[3]}a_{12} + \frac{[6][2]}{[3]}a_{13} + a_{23} = 0.$$

Next we attach a \searrow on the leftmost top of webs, we have

$$0 = \begin{array}{c} \searrow \\ \text{web} \end{array} = a_{01} \begin{array}{c} \searrow \\ | \end{array} + a_{02} \begin{array}{c} \searrow \\ \diagdown \end{array} + a_{03} \begin{array}{c} \searrow \\ \diagup \end{array} + a_{12} \begin{array}{c} \searrow \\ \cup \end{array} + a_{13} \begin{array}{c} \searrow \\ \cap \end{array} + a_{23} \begin{array}{c} \searrow \\ \text{web} \end{array}$$

We find $a_{02} - [2]^2 a_{03} = 0$, $a_{12} - [2]^2 a_{13} = 0$. If we attach a \searrow on the rightmost top of webs, we have

$$0 = \begin{array}{c} \searrow \\ \text{web} \end{array} = a_{01} \begin{array}{c} \searrow \\ | \end{array} + a_{02} \begin{array}{c} \searrow \\ \diagup \end{array} + a_{03} \begin{array}{c} \searrow \\ \diagdown \end{array} + a_{12} \begin{array}{c} \searrow \\ \cup \end{array} + a_{13} \begin{array}{c} \searrow \\ \cap \end{array} + a_{23} \begin{array}{c} \searrow \\ \text{web} \end{array}$$

FIGURE 17. Useful relations of webs for Theorem 4.1.

We obtain the last two equations, $a_{01} - [2]^2 a_{02} + [2]^2 a_{03} = 0$, $[2]^2 a_{03} - [2]^2 a_{13} + a_{23} = 0$. By the normalization, we find $a_{01} = 1$. Consequently, we find all other. We can generalize this process to find the following theorem.

Theorem 4.1. *For positive integer n , the coefficient $a_{i,j}$ in the equation presented in Figure 16 is*

$$[2]^{i-j+1} \frac{[n+1][n-j+1][2n-2i+2]}{[n][2n+2][n-i+1]}.$$

Proof. To proceed the proof, we remark that the relations of webs shown in Figure 17 can be easily obtained from the relations depicted in Figure 14. Using these relations, we get the following $n-1$ equations by attaching a \cap . By attaching a \cup , we have $(n-1)^2$ equations. There are two special equations and four different shapes of equation as follows.

$$\begin{aligned} a_{n-2,n-1} + \frac{[2][6]}{[3]} a_{n-2,n} - \frac{[2][6]}{[3]} a_{n-1,n} &= 0, \\ -\frac{[2][6]}{[3]} a_{12} + \frac{[2][6]}{[3]} a_{13} + a_{23} + 1 + \frac{[2][6]}{[3]} b_2 - [2][4] b_3 &= 0. \end{aligned}$$

Type I : For $i = 1, 2, \dots, n-3$,

$$a_{i,i+1} + \frac{[2][6]}{[3]} a_{i,i+2} - [2][4] a_{i,i+3} - \frac{[2][6]}{[3]} a_{i+1,i+2} + \frac{[2][6]}{[3]} a_{i+1,i+3} + a_{i+2,i+3} = 0.$$

Type II : For $i = 0, 1, \dots, n-2$,

$$a_{i,n-1} - [2]^2 a_{i,n} = 0.$$

Type III : For $i = 0, 1, 2, \dots, n-3$, $k = 2, 3, \dots, n-i-1$,

$$a_{i,n-k} - [2]^2 a_{i,n-k+1} + [2]^2 a_{i,n-k+2} = 0.$$

Type IV : For $i = 3, 4, \dots, n$, $k = n-i+3, n-i+4, \dots, n$,

$$[2]^2 a_{n-k,i} - [2]^2 a_{n-k+1,i} + a_{n-k+2,i} = 0.$$

Then we check our answer satisfies the equations. Since these webs in the equation depicted in Figure 16 form a basis, the coefficients are unique. Therefore, it completes the proof. \square

$$\begin{array}{c} n \\ | \\ \text{---} \\ | \\ n \end{array} = \sum_{i=0}^{n-1} \sum_{j=i+1}^n a_{ij} \begin{array}{c} j \quad i \\ \text{---} \\ | \\ n-1 \end{array}$$

FIGURE 18. A single clasp expansion of the clasp of weight $(0, n)$.

By attaching the clasp of weight $(n-1, 0)$ on the top of all webs in the equation presented in Figure 16, we find the double clasp expansion of the clasp of weight $(n, 0)$.

Corollary 4.2. *For positive integer n ,*

$$\begin{array}{c} n \\ | \\ \text{---} \\ | \\ n \end{array} = \begin{array}{c} n-1 \\ | \\ \text{---} \\ | \\ n-1 \end{array} + \frac{[2n][n+1][n-1]}{[2n+2][n][n]} \begin{array}{c} n-1 \\ | \\ \text{---} \\ | \\ n-1 \end{array} + \frac{[n-1]}{[n][2]} \begin{array}{c} n-1 \\ | \\ \text{---} \\ | \\ n-1 \end{array}$$

Then we look at the clasp of weight $(0, n)$. The main idea for the clasp of weight $(n, 0)$ works exactly same except we replace the basis as in Figure 18. As we did for the clasp of weight $(n, 0)$, we first find the equations in Figure 19 for the next step. By attaching a \cap and a \cup , we get the following equations and we can solve them successively as in Theorem 4.3.

$$a_{n-2, n-1} - [5][2]^2 a_{n-2, n} + \frac{[6][5]}{[3][2]} a_{n-1, n} = 0,$$

$$-[3][2]^2 a_{n-2, n} + [5] a_{n-1, n} = 0.$$

Type I : For $i = 0, 1, \dots, n-3$,

$$a_{i, i+1} - [5][2]^2 a_{i, i+2} + [3][2]^4 a_{i, i+3} + \frac{[6][5]}{[3][2]} a_{i+1, i+2} - [5][2]^2 a_{i+1, i+3} + a_{i+2, i+3} = 0$$

Type II : For $i = 0, 1, \dots, n-2$,

$$a_{i, n-1} - [4][2] a_{i, n} = 0.$$

Type III : For $i = 0, 1, \dots, n-3$ and $j = i+1, i+2, \dots, n-2$,

$$a_{i, j} - [4][2] a_{i, j+1} + [2]^4 a_{i, j+2} = 0.$$

Type IV : For $i = 0, 1, \dots, n-3$ and $j = i+3, i+4, \dots, n$,

$$[2]^4 a_{i, j} - [4][2] a_{i+1, j} + a_{i+2, j} = 0.$$

Type V : For $i = 1, 2, \dots, n-2$

$$-[3][2]^2 a_{i-1, i+1} + [2]^4 a_{i-1, i+2} + [5] a_{i, i+1} - [3][2]^2 a_{i, i+2} = 0.$$

$$\begin{aligned}
\text{Cup} &= [5] \quad , \quad \text{Cap} = -[2]^2[5] \\
\text{Crossing} &= -[2][4] \text{ (Y-shape)} - [2]^2[3] \text{ (X-shape)} \\
\text{Double Crossing} &= -[2][4] \text{ (X-shape)} + [2]^4[3] \text{ (X-shape)}
\end{aligned}$$

FIGURE 19. Useful relations of webs for Theorem 4.3.

Theorem 4.3. *For positive integer n , the coefficient $a_{i,j}$ in the equation presented in Figure 18 is*

$$[2]^{2(1+i-j)} \frac{[2n+1-2i][2n-2j+2]}{[2n][2n+1]}.$$

By attaching the clasp of weigh $(0, n-1)$ on the top of all webs shown in Figure 18 we find the double clasps expansion of the clasp of weight $(0, n)$.

Corollary 4.4. *For positive integer n ,*

$$\begin{aligned}
\text{Clasp}(n) &= \text{Clasp}(n-1) + \frac{[2n-1][2n-2]}{[2n+1][2]} \text{Clasp}(n-2) + \frac{[2n-2]}{[2n][2][2]} \text{Clasp}(n-1)
\end{aligned}$$

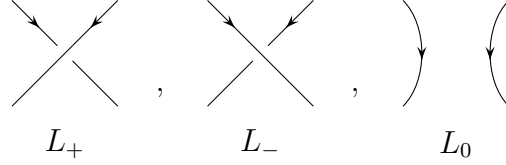
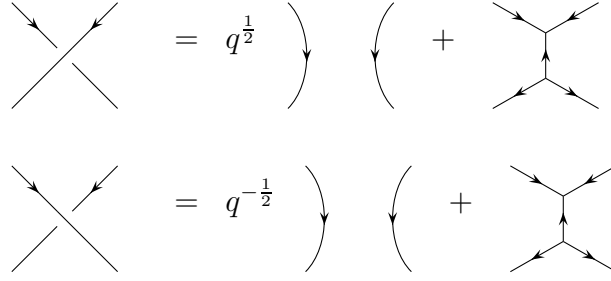
5. APPLICATIONS OF THE QUANTUM $\mathfrak{sl}(3)$ REPRESENTATION THEORY

In the section we will discuss some applications of the quantum $\mathfrak{sl}(3)$ representation theory.

5.1. Polynomial invariants of links. The HOMFLY polynomial $P_3(q)$ can be obtained by coloring all components by the vector representations of the quantum $\mathfrak{sl}(3)$ and the following skein relations

$$\begin{aligned}
P_3(\emptyset) &= 1, \\
P_3(\bigcirc \cup D) &= [3]P_3(D), \\
q^{\frac{3}{2}}P_3(L_+) - q^{-\frac{3}{2}}P_3(L_-) &= (q^{\frac{1}{2}} - q^{-\frac{1}{2}})P_3(L_0),
\end{aligned}$$

where \emptyset is the empty diagram, \bigcirc is the trivial knot and L_+, L_- and L_0 are three diagrams which are identical except at one crossing as in Figure 20. On the other hand, the polynomial $P_3(q)$ can be computed by linearly expanding each crossing into a sum of webs as in Figure 21 then by applying relations in Figure 5 [1, 15, 26]. A benefit of using webs is that we can easily define the colored $\mathfrak{sl}(3)$ HOMFLY polynomial $G_3(L, \mu)$ of L as follows. Let L be a colored link of l components say, L_1, L_2, \dots, L_l , where each component L_i is colored by an irreducible representation $V_{a_i\lambda_1+b_i\lambda_2}$ of the quantum $\mathfrak{sl}(3)$ and λ_1, λ_2 are the fundamental weights of $\mathfrak{sl}(3)$.

FIGURE 20. The shape of L_+ , L_- and L_0 .FIGURE 21. Expansion of crossings for $P_3(q)$.

The coloring is denoted by $\mu = (a_1\lambda_1 + b_1\lambda_2, a_2\lambda_1 + b_2\lambda_2, \dots, a_l\lambda_1 + b_l\lambda_2)$. First we replace each component L_i by $a_i + b_i$ copies of parallel lines and each of a_i lines is colored by the weight λ_1 and each of b_i lines is colored by the weight λ_2 . Then we put a clasp of the weight $(a_i\lambda_1 + b_i\lambda_2)$ for L_i . If we assume the clasps are far away from crossings, we expand each crossing as in Figure 21, then expand each clasp inductively by Theorem 3.4. The value we find after removing all faces by using the relations in Figure 5 is the colored $\mathfrak{sl}(3)$ HOMFLY polynomial $G_3(L, \mu)$ of L . One can find the following theorem which is a generalization of a criterion to determine the periodicity of a link [1, 3].

Theorem 5.1. *Let p be a positive integer and L be a p -periodic link in S^3 with the factor link \bar{L} . Let μ be a p -periodic coloring of L and $\bar{\mu}$ be the induced coloring of \bar{L} . Then*

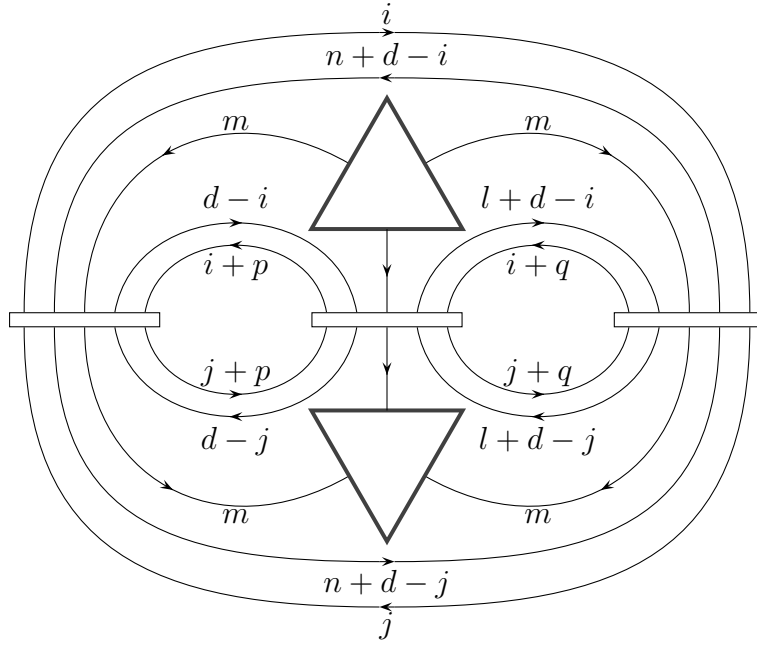
$$G_3(L, \mu) \equiv G_3(\bar{L}, \bar{\mu})^p \quad \text{modulo } \mathcal{I}_3,$$

where \bar{L} is the factor link and \mathcal{I}_3 is the ideal of $\mathbb{Z}[q^{\pm\frac{1}{2}}]$ generated by p and $[3]^p - [3]$.

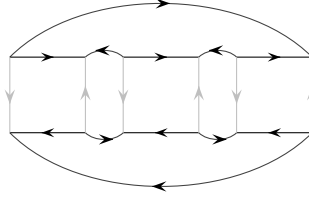
Proof. Since the clasps are idempotents, for each component, we put $p - 1$ extra clasps for each copies of components by the rotation of order p . First we keep the clasps far away from the crossings. The key idea of the proof given in [1] is that if any expansion of crossings occurs in the link diagram, it must be used identically for all other $p - 1$ copies of the diagram. Otherwise there will be p identical shapes by the rotation of order p , then it is congruent to zero modulo p . By the same philosophy, if any application of relations occurs, it must be used identically for all other $p - 1$ copies. Otherwise it is congruent to zero modulo p . Once there is an unknot in the fundamental domain of the action of order p , there are p identical unknots by the rotation which occurs only once in the factor link. Therefore, we get the congruence $[3]^p - [3]$. \square

5.2. $3j$ and $6j$ symbols for the quantum $\mathfrak{sl}(3)$ representation theory. $3j$ symbols and $6j$ symbols for the quantum $\mathfrak{sl}(2)$ representation theory have many significant implications in

$$\begin{array}{c} a \\ \circ \quad \circ \\ b \\ \circ \quad \circ \\ c \end{array} = \left[\begin{array}{c} \text{trihedron with faces } i, j, k \end{array} \right] = (-1)^{i+j+k} \frac{[i+j+k+1]![i]![j]![k]!}{[i+j]![j+k]![i+k]!}.$$

FIGURE 22. Trihedron coefficients for $\mathfrak{sl}(2)$.FIGURE 23. General shape of $\Theta(a_1, b_1, a_2, b_2, a_3, b_3; i, j)$

Mathematics and Physics. $3j$ symbols are given in the equation shown in Figure 22 [27]. Its natural generalization for the quantum $\mathfrak{sl}(3)$ representation theory was first suggested [16] and studied [14]. Let λ_1, λ_2 be the fundamental dominant weights of $\mathfrak{sl}(3, \mathbb{C})$. Let $V_{a\lambda_1+b\lambda_2}$ be an irreducible representation of $\mathfrak{sl}(3, \mathbb{C})$ of highest weight $a\lambda_1 + b\lambda_2$. Now each edge of Θ is decorated by an irreducible representation of $\mathfrak{sl}(3)$, let say $V_{a_1\lambda_1+b_1\lambda_2}$, $V_{a_2\lambda_1+b_2\lambda_2}$ and $V_{a_3\lambda_1+b_3\lambda_2}$ where a_i, b_j are nonnegative integers. Let $d = \min \{a_1, a_2, a_3, b_1, b_2, b_3\}$. If $\dim(\text{Inv}(V_{a_1\lambda_1+b_1\lambda_2} \otimes V_{a_2\lambda_1+b_2\lambda_2} \otimes V_{a_3\lambda_1+b_3\lambda_2}))$ is nonzero, in fact $d+1$, then we say a triple of ordered pairs $((a_1, b_1), (a_2, b_2), (a_3, b_3))$ is *admissible*. One can show $((a_1, b_1), (a_2, b_2), (a_3, b_3))$ is admissible if and only if there exist nonnegative integers k, l, m, n, o, p, q such that $a_2 = d + l + p$, $a_3 = d + n + q$, $b_1 = d + k + p$, $b_2 = d + m + q$, $b_3 = d + o$ and $k - n = o - l = m$. For an admissible triple, we can write its trihedron coefficients as a $(d+1) \times (d+1)$ matrix. Let us denote it by $M_\Theta(a_1, b_1, a_2, b_2, a_3, b_3)$ or $M_\Theta(\lambda)$ where $\lambda = a_1\lambda_1 + b_1\lambda_2 + a_2\lambda_1 + b_2\lambda_2 + a_3\lambda_1 + b_3\lambda_2$. Also we denotes its (i, j) entry by $\Theta(a_1, b_1, a_2, b_2, a_3, b_3; i, j)$ or $\Theta(\lambda; i, j)$ where $0 \leq i, j \leq d$. The trihedron shape of $\Theta(a_1, b_1, a_2, b_2, a_3, b_3; i, j)$ is given in Figure 23 where the triangles are filled by cut outs from the hexagonal tiling

FIGURE 24. Prime web 6_1 .

of the plane [16]. $M_\Theta(0, m+n, l, m+q, n+q, m+l)$, $M_\Theta(0, n+p, p+l, q, n+q, l)$ and $M_\Theta(i, j+k, k+l, m, j+m, j+l; 0, 0)$ were found in [14]. All other cases of $3j$ symbols and $6j$ symbols are left open.

5.3. $\mathfrak{sl}(3)$ invariants of cubic planar bipartite graphs. The $\mathfrak{sl}(3)$ webs are directed cubic bipartite planar graphs together circles (no vertices) where the direction of the edges is from one set to the other set in the bipartition. From a given directed cubic bipartite planar graph, we remove all circles by the relation 1 and then remove the multiple edges by the relation 2 in Figure 5. Using a simple application of the Euler characteristic number of a graphs in the unit disc, we can show the existence of a rectangular face [28]. By inducting on the number of faces, we provides the existence of the quantum $\mathfrak{sl}(3)$ invariants of directed cubic bipartite planar graphs. It is fairly easy to prove the quantum $\mathfrak{sl}(3)$ invariant does not depend on the choice of directions in the bipartition. Thus, the quantum $\mathfrak{sl}(3)$ invariant naturally extends to any cubic bipartite planar graph G , let us denote it by $P_G(q)$. By using a favor of graph theory, we find a classification theorem and provide a method to find all 3-connected cubic bipartite planar graphs which is called *prime webs* [17]. As little as it is known about the properties of the quantum invariants of links, we know a very little how $P_G(q)$ tells us about the properties of graphs.

For symmetries of cubic bipartite planar graph, the idea of the Theorem 5.1 and 5.3 works for the $\mathfrak{sl}(3)$ graph invariants with one exception. There is a critical difference between these two invariants which is illustrated in Theorem 5.2.

Theorem 5.2. [17] *Let G be a planar cubic bipartite graph with the group of symmetries Γ of order n . Let Γ_d be a subgroup of Γ of order d such that the fundamental domain of G/Γ_d is not a basis web with the given boundary. Then*

$$P_G(q) \equiv (P_{G/\Gamma_d}(q))^d \quad \text{modulo } \mathcal{I}_d,$$

where \mathcal{I}_d is the ideal of $\mathbb{Z}[q^{\pm\frac{1}{2}}]$ generated by d and $[3]^d - [3]$.

If the fundamental domain of G/Γ is a basis web with the given boundary, then the main idea of the theorem no longer works and a counterexample was found as follows [17]. We look at an example 6_1 as shown in Figure 24. By a help of a machine, we can see that there does not exist an $\alpha \in \mathbb{Z}[q^{\pm\frac{1}{2}}]$ such that

$$(\alpha)^6 \equiv [2]^4[3] + 2[2]^2[3] \pmod{\mathcal{I}_6}$$

even though there do exist a symmetry of order 6 for 6_1 .

5.4. Applications for the quantum $\mathfrak{sp}(4)$ representation theory. A quantum $\mathfrak{sp}(4)$ polynomial invariant $G_{\mathfrak{sp}(4)}(L, \mu)$ can be defined [15, 16] where μ is a fundamental representation of the quantum $\mathfrak{sp}(4)$. Since we have found single clasp expansion of the clasps of

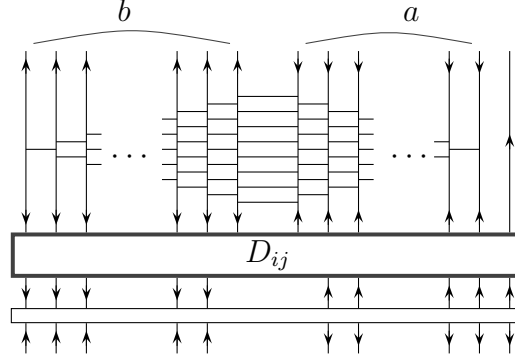


FIGURE 25. A sequence of H 's which transforms D_{ij} to a linear combinations of webs in the single clasp expansion of segregated clasp of weight $(a, b - 1)$.

weight $(a, 0)$ and $(0, b)$, we can extend $G_{\mathfrak{sp}(4)}(L, \mu)$ for μ is an irreducible representations of weight either $(a, 0)$ and $(0, b)$. If we assume a coloring $\mu = (a, 0)$ or $\mu = (0, b)$, by the same idea of the proof of Theorem 5.1, we can find the following theorem from Corollary 4.2 and 4.4.

Theorem 5.3. *Let p be a positive integer and L be a p -periodic link in S^3 with the factor link \bar{L} . Let μ be a p -periodic coloring of L and $\bar{\mu}$ be the induced coloring of \bar{L} . Then*

$$G_{\mathfrak{sp}(4)}(L, \mu) \equiv G_{\mathfrak{sp}(4)}(\bar{L}, \bar{\mu})^p \quad \text{modulo } \mathcal{I}_{\mathfrak{sp}(4)},$$

where \bar{L} is the factor link and $\mathcal{I}_{\mathfrak{sp}(4)}$ is the ideal of $\mathbb{Z}[q^{\pm \frac{1}{2}}]$ generated by p , $(-\frac{[6][2]}{[3]})^p + \frac{[6][2]}{[3]}$ and $(\frac{[6][5]}{[3][2]})^p - \frac{[6][5]}{[3][2]}$.

In fact, Theorem 5.3 remains true even if μ is any finite dimensional irreducible representation of $\mathfrak{sp}(4)$, but we would not be able to obtain the actual polynomials because any expansion is not known for the clasp of the weight (a, b) where $a \neq 0 \neq b$.

6. THE PROOF OF LEMMAS

Let us recalled that the relation 3 in Figure 5 is called a *rectangular relation* and the first(second) web in the right side of the equality is called a *horizontal(vertical, respectively) splitting*. The web in the equation shown in Figure 9 corresponding to the coefficient $a_{i,j}$ is denoted by $D_{i,j}$. After attaching H 's to $D_{i,j}$ as in Figure 25, the resulting web is denoted by $\tilde{D}_{i,j}$. We find that $\tilde{D}_{i,j}$ contains some elliptic faces. If we decompose each $\tilde{D}_{i,j}$ into a linear combination of webs which have no elliptic faces, then the union of all these webs forms a basis. Let us prove that these webs actually form a basis which will be denoted by $D'_{i',j'}$. As vector spaces, this change, adding H 's as in Figure 25, induces an isomorphism between two web spaces because its matrix representation with respect to these web bases $\{D_{i,j}\}$ and $\{D'_{i',j'}\}$ is an $(a+1)b \times (a+1)b$ matrix whose determinant is $\pm[2]^{ab}$ because a single H contributes $\pm[2]$ depends on the choice of the direction of H .

To find a single clasp expansion of the segregated clasp of weight (a, b) , we have to find all linear expansions of $\tilde{D}_{i,j}$ into a new web basis $D'_{i',j'}$. In general this is very complicate. Instead of using relations for linear expansions, we look for an alternative. From $\tilde{D}_{i,j}$ we see that there are $a+b+1$ nodes on top and $a+b-1$ nodes right above the clasp. A Y shape in

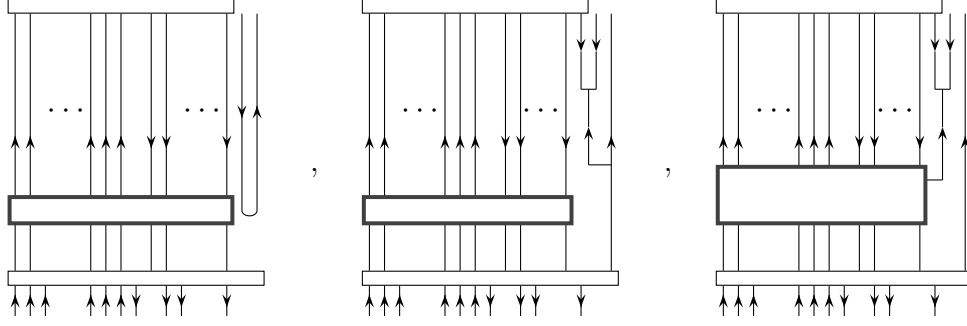


FIGURE 26. Three webs which do not vanish after attaching the clasp of weight $(a, b-1)$ to the top left side of webs $\tilde{D}_{i,j}$ from the equation in Figure 25.

the web $D_{i,j}$ forces $\tilde{D}_{i,j}$ to have at least one rectangular face. Each splitting creates another rectangular face until it becomes a basis web (possibly using the relation 2 in Figure 5 once). If we repeatedly use the rectangular relations as in equation 3 in Figure 5, we can push up Y 's so that there are either two Y 's or one U shape at the top. A *stem* of a web is $a+b-1$ disjoint union of vertical lines which connect top $a+b-1$ nodes out of $a+b+1$ nodes to the clasp of weight $(a, b-1)$ together a U -turn or two Y 's on top. It is clear that these connecting lines should be mutually disjoint, otherwise, we will have a cut path with weight less than $(a, b-1)$, *i.e.*, the web is zero. Unfortunately some of stems do not arise naturally in the linear expansion of $\tilde{D}_{i,j}$ because it may not be obtained by removing elliptic faces. If a stem appears, we call it an *admissible stem*. For single clasp expansions, finding all these admissible stems will be more difficult than linear expansions by relations. But for double clasp expansions of segregated clasps of weight (a, b) there are only few possible admissible stems whose coefficients are nonzero.

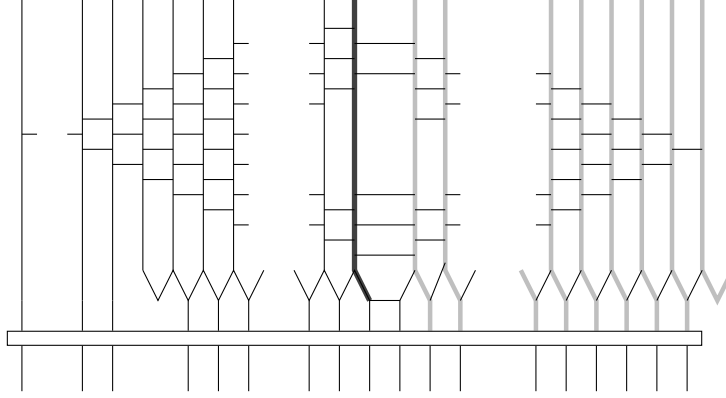
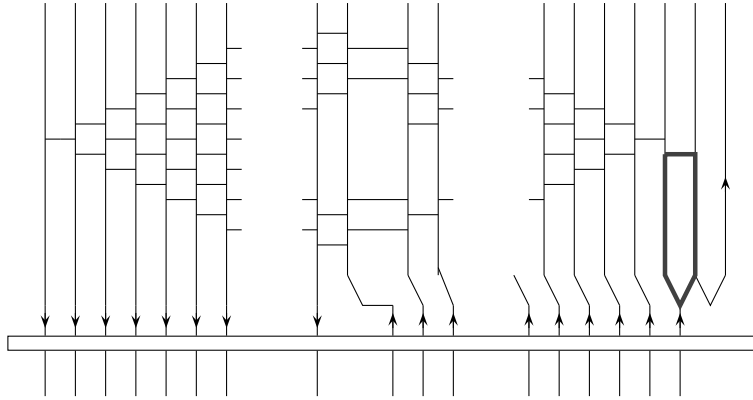
Lemma 6.1. *After attaching the clasp of weight $(a, b-1)$ to the top left side of webs $\tilde{D}_{i,j}$ from the equation in Figure 25, the only non-vanishing webs are those three webs in Figure 26.*

Proof. It is possible to have two adjacent Y 's which appear in the second and third webs in Figure 26 but a U -turn can appear in only two places because of the orientation of edges. If we attach the clasp of weight $(a, b-1)$ to the northwest corner of the resulting web and if there is a U or a Y shape just below the clasp of weight $(a, b-1)$, the web becomes zero. Therefore only these three webs do not vanish. \square

In the following lemma, we find all $\tilde{D}_{i,j}$'s which can be transformed to each of the web in Figure 26.

Lemma 6.2. *Only $\tilde{D}_{1,a}(\tilde{D}_{2,a})$ can be transformed to the first(second, respectively) web in Figure 26. Only the three webs, $\tilde{D}_{1,a-1}, \tilde{D}_{1,a}$ and $\tilde{D}_{2,a-1}$ can be transformed to the last web. Moreover, all of these transformations use only rectangular relations as in equation 3 except the transformation from $\tilde{D}_{1,a-1}$ to the third web uses the relation 2 in Figure 5 exactly once.*

Proof. For the first web in Figure 26, it is fairly easy to see that we need to look at $\tilde{D}_{i,a}$, for $i = 1, 2, \dots, b$, otherwise the last two strings can not be changed to the first web in Figure 26 with a U -turn. Now we look at the $D_{i,a}$ where $i > 1$ as in Figure 27. Since we picked where

FIGURE 27. $D_{i,a}$ where $i > 1$.FIGURE 28. The web $\tilde{D}_{1,a}$.

the U turn appears already, only possible disjoint lines are given as thick and lightly shaded lines but we can not finish to have a stem because the darkly shaded string from the left top can not be connected to the bottom clasp without being zero, *i.e.*, if we connect the tick line to clasp, there will be either \wedge or a \cap right above of the clasp of weight $(a, b - 1)$.

So only nonzero admissible stems should be obtained from $\tilde{D}_{1,a}$. As we explained before, one can see that there is a rectangular face in the web $\tilde{D}_{1,a}$. Since the horizontal splitting makes it zero, we have to split vertically. For the resulting web, this process created one rectangular face at right topside of previous place. We have to split vertically and the process are repeated until the last step, both splits do not vanish. The web in the last step is drawn in Figure 28 with the rectangular face, darkly shaded. The vertical split gives us the first web in Figure 26 and the horizontal split gives the third web in Figure 26.

A similar argument works for the second one in Figure 26. The third web in Figure 26 is a little subtle. First one can see that none of $\tilde{D}_{i,j}$ can be transformed if either $i > 2$ or $j < a - 1$. Thus, we only need to check $\tilde{D}_{1,a-1}$, $\tilde{D}_{1,a}$, $\tilde{D}_{2,a-1}$ and $\tilde{D}_{2,a}$ but we already know about $\tilde{D}_{1,a}$, $\tilde{D}_{2,a}$. Figure 29 shows the nonzero admissible stem for $\tilde{D}_{1,a-1}$. As usual, we draw a stem as a union of thick and darkly shaded lines. Note that we have used relation 3 in

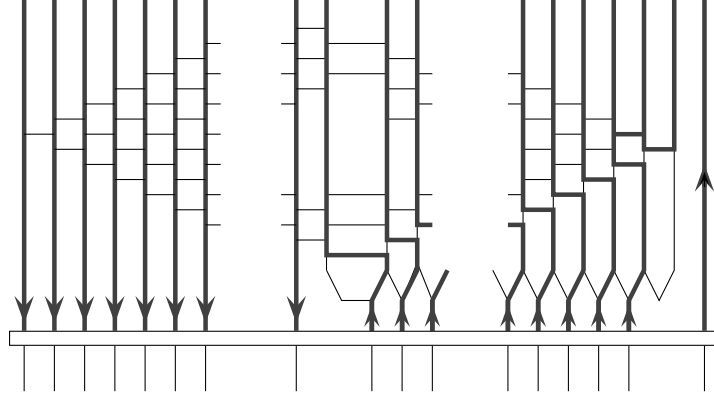
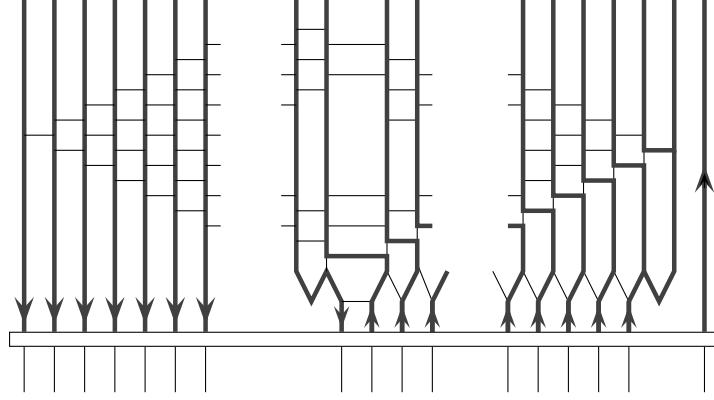
FIGURE 29. The nonzero admissible stem for $\tilde{D}_{1,a-1}$.FIGURE 30. The nonzero admissible stem for $\tilde{D}_{2,a-1}$.

Figure 5 exactly once which contributes $-[2]$. The Figure 30 shows the nonzero admissible stem for $\tilde{D}_{2,a-1}$. This completes the proof of the lemma. \square

REFERENCES

1. N. Chbili, *The quantum $SU(3)$ invariant of links and Murasugi's congruence*, Topology appl., 122 (2002), 479–485.
2. N. Chbili, *Quantum invariants and finite group actions on three-manifolds*, preprint, arXiv:math.QA/0310459.
3. Q. Chen and T. Le, *Quantum invariants and periodic links and periodic manifolds*, preprint, arXiv:math.QA/0408358.
4. W. Fulton and J. Harris, *Representation theory*, Graduate Texts in Mathematics, 129, Springer-Verlag, New York-Heidelberg-Berlin, 1991.
5. I. Frenkel and M. Khovanov, *Canonical bases in tensor products and graphical calculus for $U_q(\mathfrak{sl}_2)$* , Duke Math. J., 87(3) (1997), 409–480.
6. S. Garoufalidis and T. Le, *Is the Jones polynomial of a knot really a polynomial?*, preprint, arXiv:math.GT/0601139.
7. J. Humphreys, *Introduction to Lie algebras and representation theory*, Graduate Texts in Mathematics, 9, Springer-Verlag, New York-Heidelberg-Berlin, 1972.
8. V. F. R. Jones, *Index of subfactors*, Invent. Math., 72 (1983), 1–25.

9. V. F. R. Jones, *Polynomial invariants of knots via von Neumann algebras*, Bull. Amer. Math. Soc., 12 (1985), 103–111.
10. M. Jeong and D. Kim, *Quantum $\mathfrak{sl}(n)$ link invariants*, preprint, arXiv:math.GT/0506403.
11. M. Khovanov, *Categorifications of the colored Jones polynomial*, J. Knot Theory Ramifications, 14 (1) (2005) 111–130, arXiv:math.QA/0302060.
12. M. Khovanov, *$sl(3)$ link homology*, Algebr. Geom. Topol., 4 (2004), 1045–1081.
13. D. Kim, *Graphical Calculus on Representations of Quantum Lie Algebras*, Thesis, UC Davis, 2003, arXiv:math.QA/0310143.
14. D. Kim, *Trihedron coefficients for $\mathcal{U}_q(\mathfrak{sl}(3))$* , to appear in J. Knot theory Ramifications.
15. G. Kuperberg, *The quantum G_2 link invariant*, Int. J. Math. 5(6) (1994), 61–85.
16. G. Kuperberg, *Spiders for rank 2 Lie algebras*, Comm. Math. Phys., 180(1) (1996), 109–151, arXiv:q-alg/9712003.
17. D. Kim and J. Lee, *The quantum $\mathfrak{sl}(3)$ invariants of cubic bipartite planar graphs*, preprint.
18. M. Khovanov and G. Kuperberg, *Web bases for $sl(3)$ are not dual canonical*, Pacific J. Math., 188(1) (1999), 129–153, arXiv:q-alg/9712046.
19. D. Kim and G. Kuperberg, *Invariant tensors for the representations of $\mathfrak{sl}(4)$* , preprint.
20. R. Kirby and P. Melvin, *The 3-manifold invariants of Witten and Reshetikhin-Turaev for $\mathfrak{sl}(2, \mathbb{C})$* , Invent. Math., 105, (1991), 473–545.
21. M. Khovanov and L. Rozansky, *Matrix factorizations and link homology*, preprint, arXiv:QA/0401268.
22. T. Le, *Integrality and symmetry of quantum Link invariants*, Duke Math. J., 102 (2000), 273–306.
23. W. Lickorish, *Distinct 3-manifolds with all $SU(2)_q$ invariants the same*, Proc. Amer. Math. Soc., 117 (1993), 285–292.
24. W. Lickorish, *The skein method for three manifold invariants*, J. Knot theory Ramifications, 2 (1993), 171–194.
25. H. Murakami, *Asymptotic Behaviors of the colored Jones polynomials of a torus knot*, Internat. J. Math., 15(6) (2004), 547–555, arXiv:math.GT/0405126.
26. H. Murakami and T. Ohtsuki and S. Yamada, *HOMFLY polynomial via an invariant of colored plane graphs*, L'Enseignement Mathématique, t., 44 (1998), 325–360.
27. G. Masbaum and P. Vogel, *3-valent graphs and the Kauffman bracket*, Pacific J. Math., 164 (1994), 361–381.
28. T. Ohtsuki and S. Yamada, *Quantum $su(3)$ invariants via linear skein theory*, J. Knot Theory Ramifications, 6(3) (1997), 373–404.
29. T. Van Zandt. PSTricks: PostScript macros for generic \TeX . Available at `ftp://ftp.princeton.edu/pub/tvz/`.
30. N. Yu. Reshetikhin and V. G. Turaev, *Ribbob graphs and their invariants derived from quantum groups*, Comm. Math. Phys., 127 (1990), 1–26.
31. N. Yu. Reshetikhin and V. G. Turaev, *Invariants of 3-manifolds via link polynomials and quantum groups*, Invent. Math., 103 (1991), 547–597.
32. G. Rumer, E. Teller and H. Weyl., *Eine für die Valenztheorie geeignete Basis der binären Vektorinvarianten.*, Nachr. Ges. Wiss. gottingen Math.-Phys. Kl., (1932) 499–504.
33. M. Sokolov, *On the absolute value of the $SO(3)$ -invariant and other summands of the Turaev-Viro invariant*, Banach Center Publ., 42, Polish Acad. Sci. Knot theory (Warsaw, 1995), (1998), 395–408, arXiv:q-alg/9601013.
34. M. Sokolov, *Skein theory for $SU(n)$ -quantum invariants*, preprint, arXiv:math.QA/0407299.
35. M. Vybornov, *Solutions of the Yang-Baxter equation and quantum $\mathfrak{sl}(2)$* , J. Knot Theory Ramifications, 8(7) (1999), 953–961, arXiv:math.QA/9806058.
36. H. Wenzl, *On sequences of projections*, C. R. Math. Rep. Acad. Sci. R. Can IX (1987), 5–9.
37. B. Westbury, *Invariant tensors for the spin representation of $\mathfrak{so}(7)$* , arXiv:math.QA/0601209.
38. E. Witten, *Quantum field theory and the Jones polynomial*, Commun. Math. Phys., 121 (1989), 300–379.
39. Y. Yokota, *Skein and quantum $SU(N)$ invariants of 3-manifolds*, Math. Ann., 307 (1997), 109–138.

DEPARTMENT OF MATHEMATICS, KYUNGPOOK NATIONAL UNIVERSITY, TAEGU 702-201 KOREA
 E-mail address: dongseok@yumail.ac.kr